Observation of the Dynamical Structure of Turbulence in Plasma Confined by a Dipole Magnetic Field

B. A. Grierson,* M. W. Worstell, and M. E. Mauel

Department of Applied Physics and Applied Mathematics,

Columbia University, New York, NY 10027 USA

(Dated: October 14, 2008)

Abstract

Steady state interchange-like electrostatic turbulence, produced in a plasma confined by a strong dipole magnet, is observed to be dominated by a limited number of low-order, rotating azimuthal modes which vary irregularly in time and cause chaotic plasma fluctuations. The predominance of large scale structures represents the "self-organized" state of dipole-confined plasma turbulence and is attributed to a nonlinear inverse energy cascade and a linear damping of small scale structures.

PACS numbers: 52.35Mw, 52.35.Ra, 52.55.Hc

Fluid and plasma turbulence results from complex, nonlinear phenomena that couples structures at different scales. Understanding the spatial and temporal characteristics of the turbulent fluctuations remains a fundamental challenge[1, 2]. Recently, significant progress has been made through diagnostic improvements that allow observation of quasi-coherent structures and measurement of multipoint statistics of steady driven turbulence[3]. Progress has been especially rapid in certain types of strongly magnetized plasma and thin layers of fluid where the turbulent dynamics is nearly two-dimensional[4, 5]. Turbulence in two-dimensional systems is associated with an inverse energy cascade[6] that can generate self-organization at large scales and structures with long correlation lengths[7]. Quasi-two-dimensional turbulence appears to be relevant in several circumstances, and examples include plasma confined in long magnetic solenoids[8–11], in simple magnetic torii without magnetic shear[12, 13], in the scrap-off-layers of toroidal fusion confinement devices[14–16], in the solar wind[17], in magnetized columns of electrons[18, 19], and in driven thin sheets of fluid[20–22].

This Letter addresses two important questions regarding quasi-two-dimensional turbulence found in strongly magnetized plasma. What are the average local rates of linear and nonlinear energy flow associated with the turbulent spectrum? And, what are the global quasi-coherent structures that dominate the fluctuations? We answer these questions by making simultaneous measurements of both the local and global fluctuations of a plasma confined by a strong dipole magnet. Since a dipolar magnetic field has no shear, low-frequency fluctuations are electrostatic, interchange-like, and essentially two-dimensional[23]. Using a model for nonlinear power transfer[24], we find short wavelength fluctuations are damped and energy flows nonlinearly from small to large scales. Simultaneously, we observe the gross spatial and temporal fluctuations throughout the entire plasma. We find the large-scale structure of turbulence consists of rotating, long-wavelength convective cells with amplitudes that varying irregularly in time. We believe these dominant rotating global structures represent the "self-organized" state of dipole turbulence, and we attribute their appearance to an inverse energy cascade[6, 7]. Furthermore, we believe the complex temporal dynamics of the global modes result from nonlinear self-interactions[8, 25] and produce chaotic convective dynamics that should be describable by a low-dimensional model[26, 27].

Measurements were made using the Collisionless Terella Experiment (CTX), which consists of strong dipole electromagnet centered within a large 1.6 m diameter vacuum vessel.

Dipole-confined plasma with stationary turbulence is sustained by microwave heating and hydrogen gas fueling for discharges lasting up to one second. High-speed and simultaneous measurements of the fluctuations of the currents and voltages of various probe arrays and of visible light are digitally recorded at rates up to 250 ksps. The CTX device is described with detail in several references that reported measurements of centrifugally-driven interchange instability[28, 29], hot-electron driven interchange instability[30], and nonlinear phase-space dynamics due to drift-resonances with rotating interchange modes[31, 32]. Operationally, the turbulent plasma discharges reported here are obtained in the same way as described in previous studies except the level of gas fueling was doubled. This significantly increases plasma density to approximately $n_0 \sim 10^{11}$ cm^{-3} from 10^{11} cm^{-3} used in previous studies. Higher density in turn significantly reduces the production of energetic trapped electrons and stabilizes the fast hot electron interchange instability[30]. Under these conditions, the plasma exhibits strong and steady interchange turbulence that is the subject of this Letter.

The ensemble-averaged frequency spectrum of the fluctuations is measured using a single movable probe inserted into the plasma at various radii and then averaging over many hundreds of equivalent time intervals in many discharges. Fig. 1 shows the floating potential spectrum has a broad frequency band at all radii. The lower frequency range is dominated by two large-amplitude modes, one at $f \sim 1-2$ kHz and the other at $f \sim 4-6$ kHz, and we find these modes to be quasi-coherent. Above 7 kHz, the potential fluctuations have a spectrum with a power-law dependence that scales between $\sim f^{-4}$ and $\sim f^{-5}$. Fluctuations of the density measured by ion saturation current also show the quasi-coherent modes but, above 7 kHz, the ensemble-average density fluctuations have a spectrum that scales as $\sim f^{-3}$.

The turbulent fluctuations in these higher density discharges are electrostatic and interchange-like, just as they were in previously measured interchange instabilities at lower density[29, 30]. When two probes are located along the same magnetic field line, two-point correlations of the floating potential are coherent over the bandwidth of fluctuations. Additionally, the ion current fluctuations detected at two locations along the same field line are correlated, have zero phase lag, and display the same dominant frequency and power-law spectral characteristics. For example, the ion current fluctuations at a location on a pole-face of the dipole magnetic are correlated to current fluctuations detected by a Langmuir probe.

Using multiple probes around the azimuth, the cross-field, spatial coherence and az-

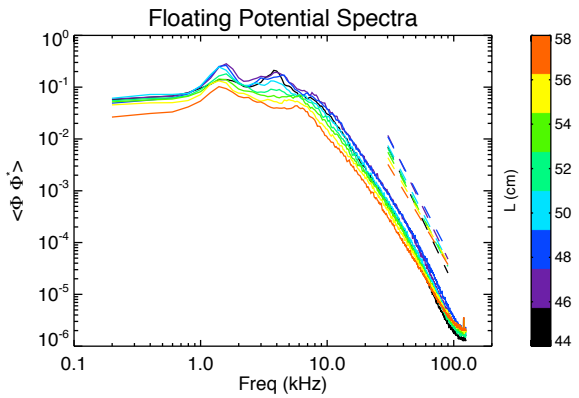

FIG. 1: Floating potential spectrum $\tilde{\Phi}_f$ as a function of equatorial radius, L, measured using a movable probe.

imuthal correlation length of the turbulence, $\delta\phi_c$, are determined. One probe is used as reference, and the ensemble cross-correlation is found between three other probes with azimuthal spatial separation of 9°, 90°, 180°. The fluctuations propagate in the direction of the average $\mathbf{E}\times\mathbf{B}$ direction, which is also the electron diamagnetic drift direction. The decrease in cross-correlation amplitude with probe separation is fit to a Gaussian, and the azimuthal correlation length of the turbulence in CTX is determined to be near $L\delta\phi_c \sim 45$ cm at an equatorial radius of $L = 50$ cm. This corresponds to $\delta\phi_c \sim 0.9$ or 14% of the device circumference. At 90° probe separation, only the low-frequency modes below 7 kHz show quasi-coherence, as shown by in Fig. 2a where the magnitude of the ensemble-averaged cross coherence of the floating potential is shown as a function of frequency.

When two probes are separated by a short distance in the azimuthal direction, $\Delta\xi = L\Delta\phi = 8$ cm, we are able to measure the local wavenumber and dispersion of the fluctuations. The average phase of the cross coherence, $\langle\alpha(\tilde{\Phi}_1, \tilde{\Phi}_2)\rangle$, is proportional to the azimuthal wavenumber, $k_\xi \approx \langle\alpha(\tilde{\Phi}_1, \tilde{\Phi}_2)\rangle/\Delta\xi$. The dispersion $k_\xi(\omega)$ is shown in Fig. 2b. The dispersion is nearly linear up to 35 kHz and corresponds to a constant phase velocity, $\omega/k_\xi \approx c \sim 2\pi$ km/sec, which we believe represents relatively rapid rotation of slowly-evolving turbulent structures. The rotation frequency is $c/2\pi L \sim 2$ kHz, comparable to the $\mathbf{E}\times\mathbf{B}$ frequency. The underlying turbulent structure evolves as it rotates and decorrelates in a time approximately $L\delta\phi_c/c \sim 70$ μsec, which is short compared to the rotation period.

The measured frequency spectra (Fig. 1) and the linear relationship between wavenumber and frequency (Fig. 2b) are consistent with Kraichnan's prediction for two-dimensional

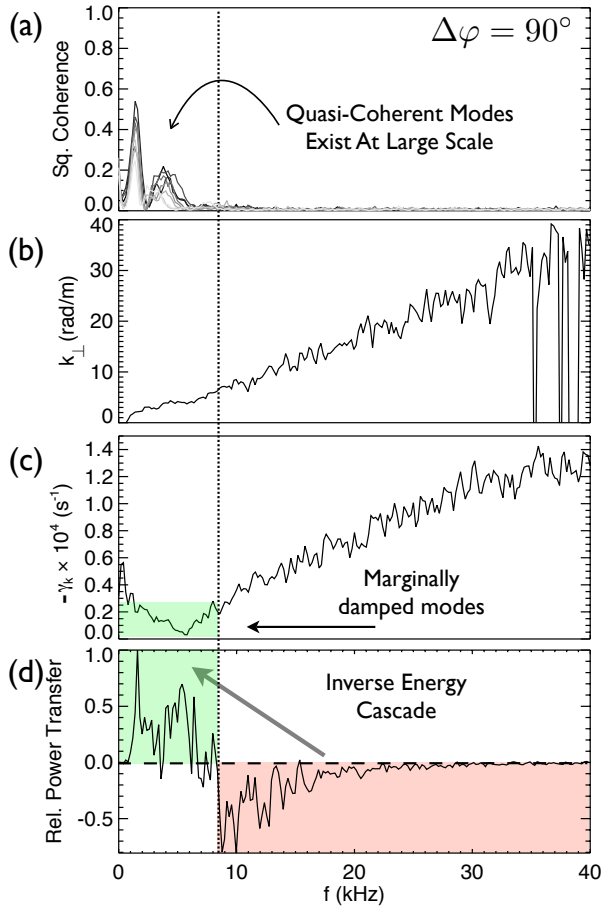

FIG. 2: Ensemble bispectral and cross-coherence analysis of the linear dispersion and nonlinear relative power transfer obtained from two-point measurements of the floating potential.

turbulence that conserves both energy and enstrophy[6]. Note that in the drift-interchange limit[7, 9], the energy contained in a low-frequency electrostatic plasma fluctuation with wavenumber k is proportional the sum of an adiabatic and an electrostatic part, or $(\tilde{n}_k/n_0)^2 + k^2\rho_s^2(e\tilde{\Phi}_k/T_e)^2$. At $L \sim 50$ cm, the total fluctuation intensity is $|\tilde{n}|/n_0 \sim 0.6$, $e|\tilde{\Phi}|/T_e \sim 0.5$, and the sonic larmor radius is $\rho_s \sim 2$ cm, with $T_e \sim 10$ eV and $|B| = 140$ G. While the adiabatic part of the fluctuation energy appears larger than the electrostatic part, when $\langle\tilde{\Phi}_k^2\rangle \sim 1/f^5$ and $\langle\tilde{n}_k^2\rangle \sim 1/f^3$, both have the same power-law dependence for the energy spectrum, which scales as the Kraichnan result, $\sim k^{-3}$, for the enstrophy cascade.

A dynamical description of the spectral energy is calculated through a statistical analysis that assumes a linear growth and dispersion and a quadratically nonlinear mode coupling term proportional to the bispectrum[24]. The fluctuations, $\tilde{\Phi}_k$, are taken to vary dynamically

according to a linear rate, $\gamma_k + i\omega_k$, and also to a nonlinear three-wave structure coupling coefficient, $\Lambda_k(k', k-k')$. The time evolution of the ensemble average of the fluctuation intensity, $\langle\tilde{\Phi}_k^2\rangle$, increases linearly as $2\gamma_k \langle\tilde{\Phi}_k^2\rangle$ and nonlinearly in proportion to the relative power transfer, defined as $\sum_{k'} \Re\{\Lambda_k(k', k-k')\}\langle\tilde{\Phi}_k^*\tilde{\Phi}_{k'}\tilde{\Phi}_{k-k'}\rangle$. Measurement of the auto- and cross-bispectrum and various cross correlations determine both the linear and nonlinear coefficients. Fig. 2c shows the fluctuation intensity damps at a rate that increases with frequency approximately as $2\gamma_k/\omega_k \approx 0.13$. For example, fluctuations at 20 kHz have a high azimuthal mode number ($m \sim 10$) and a characteristic damping time of $1/\gamma_k \approx 140$ μsec. Fluctuations with frequencies near 6 kHz are essentially undamped, and this scale may represent the turblence "source". As shown in Fig. 2d, the relative power transfer shows a net energy transfer from small scale structures with $f > 6$ kHz to the large global structures with $f < 6$ kHz. Indeed, Fig. 2 indicates that the large amplitude of the global $m = 1$ structure at 2 kHz represent nonlinear amplification due to the inverse energy casade expected for two-dimensional turbulence.

The quasi-coherent large-scale structures that comprise the "self-organized" turbulent state can be directly measured by using an array of 96 gridded particle detectors located at one pole of the dipole magnet[29]. The currents collected by all detectors are recorded simultaneously once every 4 μsec. Since the detectors are spaced more closely than a correlation length, the 96 detectors are sufficient to make high-speed images of the global dynamics of the entire plasma.

One method of viewing the polar ion current is shown in Fig. 3a where a short 8 msec record of the density fluctuations at a particular radius ($L = 50$ cm) is displayed as a function of time and azimuthal angle. The density fluctuations are dominated by rotating structures that can exists for multiple transits around the device. At each sample time, the azimuthal structure is Fourier decomposed, and the mode having the largest amplitude is indicated in Fig. 3b. For most of the second half of the time-record, a long-lived, rotating $m = 1$ structure appears and extends around the device circumference for a period much larger than the typical decorrelation time. At other times in the record, the dominate azimuthal mode can be either $m = 2$, 3, 4, or 5.

A second method to view the global structure dynamics of turbulence is the bi-orthogonal decomposition[33]. Bi-orthogonal decomposition is a tool for decomposing multiple space-time points into orthogonal spatial and orthogonal temporal mode functions using the singu-

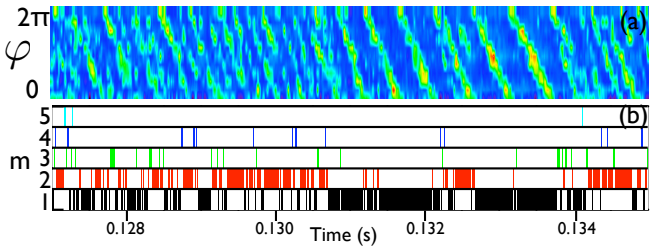

FIG. 3: (a) Density fluctuations $\tilde{n}(t, \varphi)$ in time and azimuthal angle φ, measured at one radial location. (b) Indicator of the dominant Fourier mode number.

lar value decomposition. The data provided by the polar detector array are decomposed into mode functions that are well ordered in amplitude. The spatial and temporal mode functions are dominated by the longest wavelengths and the lowest frequencies. Fig. 4 shows the result of the decomposition. The dominant spatial modes of the turbulent state are found to be spatially simple, sine and cosine functions with low-order azimuthal mode. The first two modes are the $m = 1$ sine and cosine pair, and they have nearly the same singular value due to the plasma's $\mathbf{E} \times \mathbf{B}$ rotation. The next two mode functions are the $m = 2$ sine and cosine pair that vary more quickly. Fig. 4 also shows a short 8 msec record of the temporal variations of the $m = 1$, 2, 3 modes. While the characteristic frequencies of the modes increase in proportion to m as expected, the temporal modes are highly irregular, impulsive, and bursty.

An analysis of the time series of the density fluctuations shows the density varies chaotically. The numerical Lyapunov spectrum was calculated[34] for the plasma density fluctuations obtained from the polar imager diagnostic, which provides the time series for the bi-orthogonal decomposition. A single positive Lyapunov exponent is found to converge when the embedding dimension equals three or more. A positive Lyapunov number indicates that the dynamical system has chaotic properties. This positive exponent has a characteristic time of 50 μsec, comparable to the auto-correlation time of the time series. When the embedded dimension exceeds three, the Lyapunov spectrum calculation produces small negative exponents, indicating a three-dimensional phase space is sufficient to describe the turbulent system. This result is similar to the chaotic convection motion observed in a simple shear-free magnetic torus[26]. We believe it likely that a description of the chaotic nature of convective flute motion presented by Rypdal and Garcia[27] is also applicable to the chaotic interchange dynamics in a dipole-confined plasma.

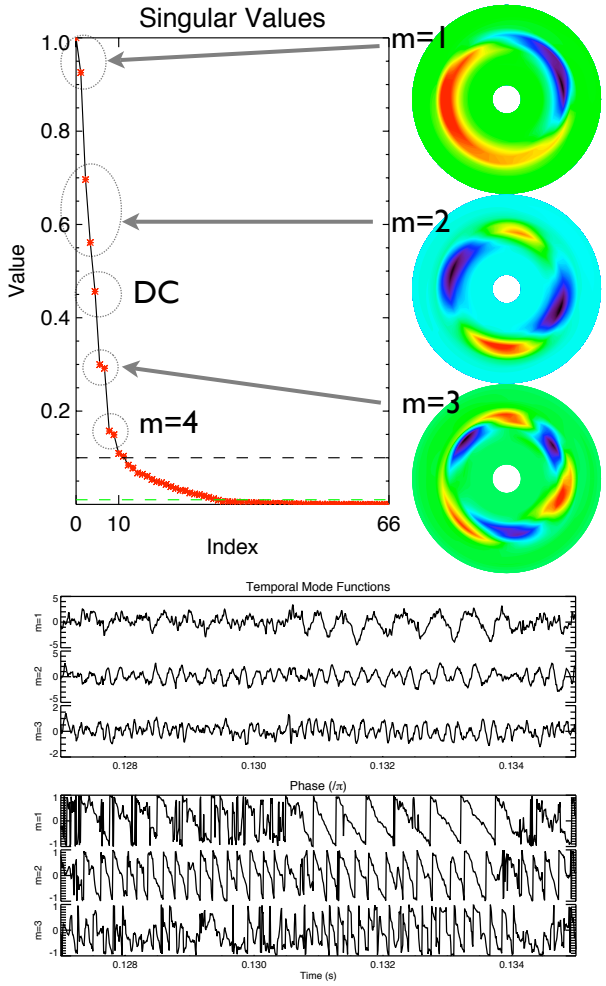

FIG. 4: Global mode structure dynamics resulting from bi-orthongal decomposition of the polar ion current measurements. Although the spatial mode functions (top) are relatively simple sinusoids, the temporal variations of the mode amplitudes and phases (bottom) are complex.

In summary, we report comprehensive measurements of the local and global structure of plasma turbulence confined by a dipole magnetic field. The spatial structure of the turbulence is dominated by long wavelength rotating structures that represent a "self-organized" state of the turbulent plasma. The global structures have complex and irregular time signatures, and the associated density fluctuations are chaotic. Ensemble-averaged spectral and bispectral analysis of the fluctuations show energy is nonlinearly transferred from short to long length scales as expected of a two-dimensional system. Other measurements and analyses support the notion that driven turbulence in dipole-confined plasma is comprised of a few dominate large-scale modes that varying chaotically in time, and these will be presented

in a longer article.

---

* Electronic address: bag2107@columbia.edu

[1] L. Kadanoff, Physics Today **54**, 34 (2001).

[2] G. Falkovich and K. Sreenivasan, Physics Today **59**, 43 (2006).

[3] R. O. Dendy and S. C. Chapman, Plasma Phys Contr F **48**, B313 (2006).

[4] P. Tabeling, Phys Rep **362**, 1 (2002).

[5] M. Shats, H. Xia, and H. Punzmann, Physical Review E **71**, 046409 (2005).

[6] R. Kraichnan, Phys Fluids **10**, 1417 (1967).

[7] A. Hasegawa, Advances in Physics **34**, 1 (1985).

[8] T. Yamada, S.-I. Itoh, T. Maruta, N. Kasuya, Y. Nagashima, S. Shinohara, K. Terasaka, M. Yagi, S. Inagaki, Y. Kawai, et al., Nat Phys p. 5 (2008).

[9] M. J. Burin, G. R. Tynan, G. Y. Antar, N. A. Crocker, and C. Holland, Phys Plasmas **12**, 052320 (2005).

[10] O. Grulke, T. Klinger, and A. Piel, Phys Plasmas **6**, 788 (1999).

[11] S. Iizuka, T. Huld, H. Pécseli, and J. Rasmussen, Phys Rev Lett **60**, 1026 (1988).

[12] K. Rypdal and S. Ratynskaia, Phys. Scr. **T122**, 52 (2006).

[13] F. Greiner, D. Block, and A. Piel, Contrib. Plasma Phys. **44**, 335 (2004).

[14] S. J. Zweben, J. A. Boedo, O. Grulke, C. Hidalgo, B. LaBombard, R. J. Maqueda, P. Scarin, and J. L. Terry, Plasma Phys Contr F **49**, S1 (2007).

[15] G. S. Xu, B. N. Wan, W. Zhang, Q. W. Yang, L. Wang, and Y. Z. Wen, Phys Plasmas **13**, 102509 (2006).

[16] M. Spolaore, V. Antoni, E. Spada, H. Bergsaker, R. Cavazzana, J. Drake, E. Martines, G. Regnoli, G. Serianni, and N. Vianello, Phys Rev Lett **93**, 215003 (2004).

[17] L. Sorriso-Valvo, R. Marino, V. Carbone, A. Noullez, F. Lepreti, P. Veltri, R. Bruno, B. Bavassano, and E. Pietropaolo, Phys Rev Lett **99**, 4 (2007).

[18] D. Durkin and J. Fajans, Phys Rev Lett **85**, 4052 (2000).

[19] K. Fine, A. Cass, W. Flynn, and C. Driscoll, Phys Rev Lett **75**, 3277 (1995).

[20] M. Rivera, W. Daniel, S. Chen, and R. Ecke, Phys Rev Lett **90**, 104502 (2003).

[21] T. Dubos, A. Babiano, J. Paret, and P. Tabeling, Physical Review E **64**, 036302 (2001).

[22] J. Paret, M. Jullien, and P. Tabeling, Phys Rev Lett **83**, 3418 (1999).

[23] A. Das, Phys Plasmas **15**, 022308 (2008).

[24] C. Ritz, E. Powers, and R. Bengtson, Physics of Fluids B: Plasma Physics **1**, 153 (1989).

[25] P. Terry, Phys Rev Lett (2004).

[26] T. Živković and K. Rypdal, Physical Review E **77**, 4 (2008).

[27] K. Rypdal and O. Garcia, Phys Plasmas (2007).

[28] B. Levitt, D. Maslovsky, and M. Mauel, Phys Rev Lett **94**, 175002 (2005).

[29] B. Levitt, D. Maslovsky, M. Mauel, and J. Waksman, Phys Plasmas **12**, 055703 (2005).

[30] B. Levitt, D. Maslovsky, and M. Mauel, Phys Plasmas **9**, 2507 (2002).

[31] H. Warren and M. Mauel, Phys Rev Lett **74**, 1351 (1995).

[32] D. Maslovsky, B. Levitt, and M. Mauel, Phys Rev Lett **90**, 185001 (2003).

[33] T. de Wit, A. Pecquet, J. Vallet, and R. Lima, Phys Plasmas **1**, 3288 (1994).

[34] J. Eckmann, S. Kamphorst, D. Ruelle, and S. Ciliberto, Physical Review A (1986).